Polarization observables in $(\vec{\gamma}, \vec{N}N)$ reactions

C. Giusti[a] and F.D. Pacati[b]

Dipartimento di Fisica Nucleare e Teorica, Università di Pavia and INFN, Sezione di Pavia, Pavia, Italy

Abstract. The formalism of $(\vec{\gamma}, \vec{N}N)$ reactions is given where the incident photon is polarized and the outgoing-nucleon polarization is detected. Sixteen structure functions and fifteen polarization observables are found in the general case, while only eight structure functions and seven polarization observables survive in coplanar kinematics. Numerical examples are presented for the ^{16}O(γ, np) and ^{16}O(γ, pp) reactions. The transitions to the ground state of ^{14}C and ^{14}N are calculated in a model where realistic short-range and tensor correlations are taken into account for the np pair, while short-range and long-range correlations are included in a consistent way for pp pairs. The effects of the one-body and two-body components of the nuclear current and the role of correlations in cross-sections and polarizations are studied and discussed.

PACS. 25.20.Lj Photoproduction reactions – 24.70.+s Polarization phenomena in reactions

1 Introduction

For a long time electromagnetically induced two-nucleon knockout has been considered the most direct tool for exploring the properties of nucleon pairs within nuclei and their interaction at short distance [1,2]. The cross-section of an exclusive reaction contains the two-hole spectral function, which gives information on nuclear structure and correlations.

Two nucleons can be naturally ejected by two-body currents, which effectively take into account the influence of subnuclear degrees of freedom like mesons and isobars. Direct insight into dynamical short-range correlations (SRC) can be obtained from the process where the real or virtual photon hits, through a one-body current, either nucleon of a correlated pair and both nucleons are then ejected from the nucleus. A reliable and consistent treatment of these two competing processes, both produced by the exchange of mesons between nucleons, is needed. Their role and relevance, however, can be different in different reactions and kinematics. It is thus possible to envisage situations where either process is dominant and various specific effects can be disentangled and separately investigated.

First pioneering (γ, NN) experiments were performed in Bonn [3] and Tokio [4] with poor statistical accuracy and energy resolution. Further experiments carried out at MAMI achieved much better results [5]. These experiments, with an energy resolution of about 6-9 MeV, were

a e-mail: giusti@pv.infn.it
b e-mail: pacati@pv.infn.it

able to resolve the major shells from which the two nucleons are emitted. The first high-resolution ^{16}O$(\gamma, np)^{14}$N experiment able to separate final states was performed at MAXlab in Lund [6]. A high-resolution experiment for the ^{16}O$(\gamma, np)^{14}$ and ^{16}O$(\gamma, pp)^{14}$C reactions in the photon-energy range between 90 and 270 MeV, aiming not only at separating final states but also at determining the momentum distributions of each state, has been recently approved in Mainz [7]. Results for a first test and feasibility study are presented in ref. [8].
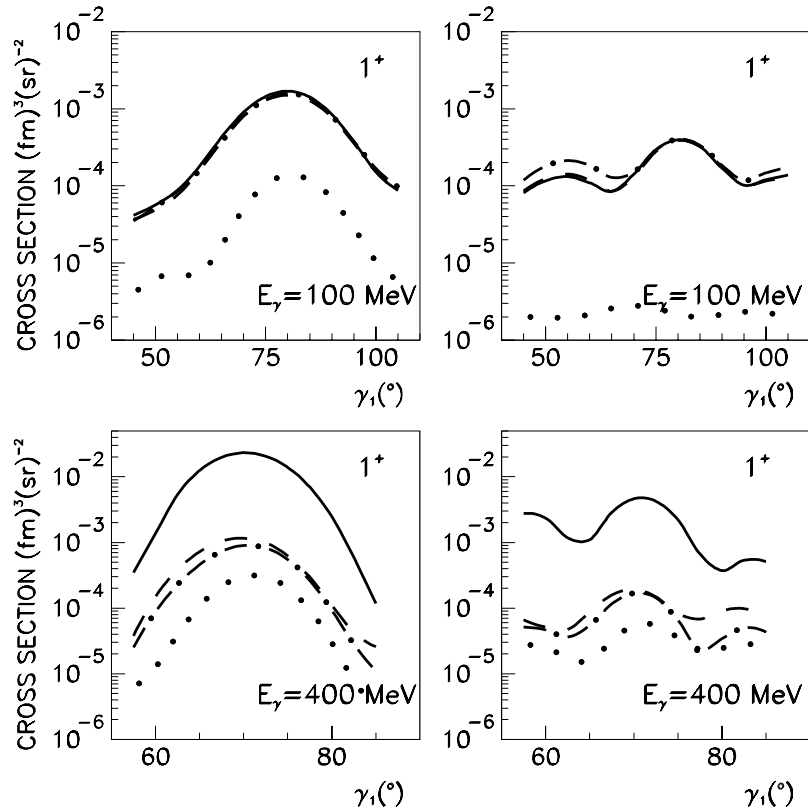
Reaction calculations performed with different microscopic models based on a two-nucleon knockout framework [9,10] confirm that (γ, np) and (γ, pp) reactions are generally dominated by two-body currents. Thus, they are useful to study the nuclear current, whose various components can be emphasized or suppressed in different conditions and kinematics. However, they are also sensitive to the other theoretical ingredients and represent a suitable tool to study the conditions of nucleon pairs within a nucleus. In fact, the angular distributions of the ^{16}O$(\gamma, np)^{14}$N and ^{16}O$(\gamma, pp)^{14}$C cross-sections for transitions to different final states have a different shape, essentially determined by the components of the center-of-mass (c.m.) orbital angular momentum of the initial pair [9], which can be explored by comparing the theoretical predictions with the experimental data.

Interesting and complementary information is available from $(e, e'NN)$ and (γ, NN) reactions. First measurements of the exclusive ^{16}O$(e, e'pp)^{14}$C reaction have been performed at NIKHEF in Amsterdam [11–13] and MAMI in Mainz [14]. Investigations on these data [11–15]

Fig. 1. The differential cross-section of the $^{16}O(\gamma, np)^{14}N_{g.s.}$ reaction as a function of the scattering angle γ_1 of the outgoing neutron in coplanar and symmetrical kinematics at $E_\gamma = 100$ MeV (upper panels) and $E_\gamma = 400$ MeV (lower panels). The two-nucleon overlap is calculated as in ref. [16] (upper panels) and as in ref. [9] (lower panels). The optical potential is taken from ref. [17]. The separate contributions given by the one-body currents (dotted lines), the sum of the one-body and seagull currents (dot-dashed lines), the sum of the one-body, seagull and pion-in-flight currents (dashed lines) are displayed. The solid lines give the final cross-sections, where also the contribution of the Δ current is added.

indicate that resolution of discrete final states provides an interesting tool to disentangle the two reaction mechanisms due to one-body currents, and thus to SRC, and to two-body currents.

Recent calculations [16] have shown that also the cross-sections of the exclusive $^{16}O(e, e'np)^{14}N$ reaction are sensitive to details of the nuclear correlations and in particular to the presence of the tensor component.

It is clear, however, that $(e, e'np)$ experiments are more difficult, as they require a triple coincidence measurement with the detection of a neutron. Thus, no data are available at present, but a proposal for the experimental study of the exclusive $^{16}O(e, e'np)^{14}N$ reaction has been approved in Mainz [18].

Good opportunities for a more complete investigation of the properties of different pairs of nucleons in nuclei and of their interaction at short distance are offered by polarization measurements. Reactions with polarized particles give access to a larger number of observables, hidden in the unpolarized case and whose determination can impose more severe constraints to theoretical models. Some of these observables are expected to be sensitive to the small components of the transition amplitudes, which are generally masked by the dominant ones in the unpolarized cross-section and that often contain interesting informa-

tion on subtle effects. In photoreactions, and in particular in (γ, np) reactions, the two-body contributions are always dominant in the cross-section with respect to one-body ones. In order to study correlations, the polarization measurements are therefore necessary.

The asymmetry of the cross-section for linearly polarized photons in (γ, pp) and (γ, np) reactions was studied in refs. [10,19]. Numerical results for exclusive pp and np knockout from ^{16}O can be found in ref. [9]. First measurements with polarized photon beams have been performed at LEGS on ^{3}He [20] and ^{16}O [21] and at MAMI on ^{12}C [22]. In these first experiments, however, the energy resolution was not enough to separate specific discrete final states of the residual nucleus.

The nucleon recoil polarization in photon-induced and electron-induced two-nucleon knockout has been considered in refs. [10] and [23], respectively. The general formalism of the $(\vec{e}, e'\vec{N}N)$ reaction and some theoretical predictions for the exclusive $^{16}O(\vec{e}, e'\vec{pp})^{14}C$ knockout reaction are given in ref. [24]. The results of these investigations indicate that a combined measurement of cross-sections and polarization components would provide an interesting tool to disentangle the different reaction mechanisms and clarify the behaviour of nucleon pairs in the nuclear
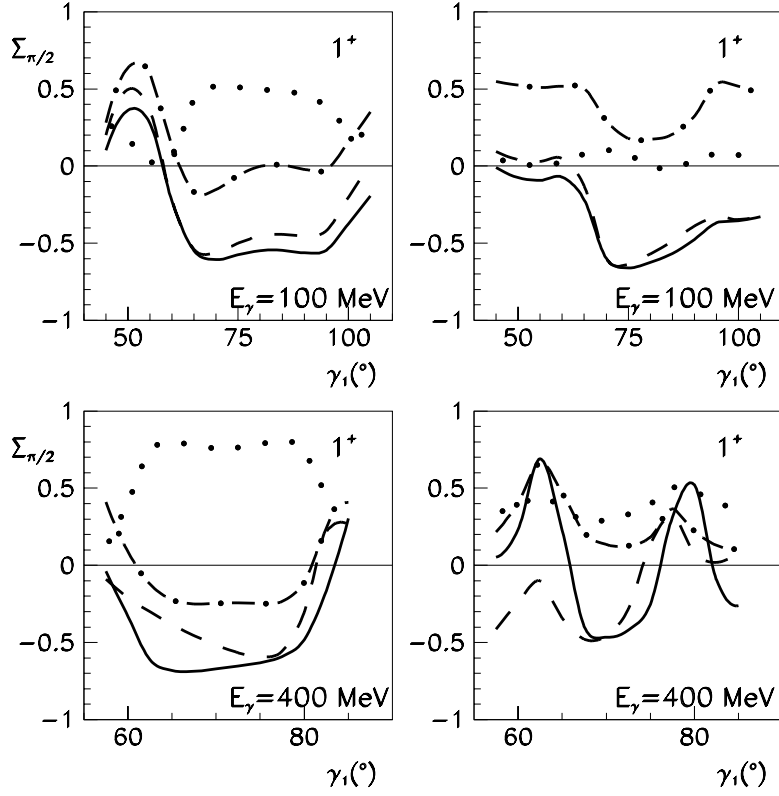
Fig. 2. The photon asymmetry of the $^{16}\text{O}(\gamma, np)^{14}\text{N}_{\text{g.s.}}$ reaction in the same kinematics and conditions and with the same line convention as in fig. 1.

medium. No data are available at present, but a measurement of the nucleon recoil polarization seems reasonably within reach of available experimental facilities.

The general case of $(\vec{\gamma}, \vec{N}N)$ reactions, where the incident photon is linearly or circularly polarized and/or the outgoing-nucleon polarization is detected is considered in this paper. Besides the cross-section, 15 new observables are obtained in the most general kinematics. The formalism and the polarization observables are given in sect. 2. Some numerical results for the exclusive $^{16}\text{O}(\vec{\gamma}, \vec{n}p)^{14}\text{N}_{\text{g.s.}}$ and $^{16}\text{O}(\vec{\gamma}, \vec{p}p)^{14}\text{C}_{\text{g.s.}}$ reactions are presented and discussed in sects. 3 and 4, respectively. Conclusions are drawn in sect. 5.

2 Polarization observables in $(\vec{\gamma}, \vec{N}N)$ reactions

The cross-section of a reaction, where an incident photon, with momentum $\boldsymbol{q}$ and energy E_γ, is absorbed by the nucleus and two nucleons are emitted, with momenta $\boldsymbol{p}'_1$ and $\boldsymbol{p}'_2$ and energies E'_1 and E'_2, can be written in terms of four structure functions $f_{\lambda\lambda'}$ as

$$\frac{\mathrm{d}^3\sigma}{\mathrm{d}\Omega_1\mathrm{d}\Omega_2\mathrm{d}E'_2} = \frac{2\pi^2\alpha}{E_\gamma}\, K[f_{11} + \Pi_{\mathrm{c}}f'_{11} - \Pi_{\mathrm{t}}(f_{1-1}\cos 2\phi_\gamma$$
$$-\bar{f}_{1-1}\sin 2\phi_\gamma)]\,, \qquad (1)$$

where Π_{c} and Π_{t} are the degrees of circular and linear polarization of the photon, ϕ_γ is the angle of the photon

polarization vector relative to the scattering plane, *i.e.* the $(\boldsymbol{q}, \boldsymbol{p}'_1)$-plane, and

$$K = |\boldsymbol{p}'_1|\, E'_1\, |\boldsymbol{p}'_2|\, E'_2\, f_{\mathrm{rec}}\,, \qquad (2)$$

with

$$f_{\mathrm{rec}}^{-1} = 1 - \frac{E'_2}{E_{\mathrm{r}}}\frac{\boldsymbol{p}'_2 \cdot \boldsymbol{p}_{\mathrm{r}}}{|\boldsymbol{p}'_2|^2}\,, \qquad (3)$$

where $\boldsymbol{p}_{\mathrm{r}}$ and E_{r} are the momentum and energy of the residual nucleus. In our reference frame the $\boldsymbol{z}$-axis is taken parallel to $\boldsymbol{q}$ and the momentum $\boldsymbol{p}'_1$ lies in the $(\boldsymbol{x}, \boldsymbol{z})$-plane.

The structure functions $f_{\lambda\lambda'}$ are obtained from the components of the hadron tensor W^{ij}, with $i, j = x, y$, and are given by all the symmetrical and antisymmetrical independent combinations of these components, *i.e.*

$$f_{11} = W^{xx} + W^{yy}, \qquad f'_{11} = -i\,(W^{xy} - W^{yx}),$$
$$f_{1-1} = W^{yy} - W^{xx}, \qquad \bar{f}_{1-1} = W^{xy} + W^{yx}. \qquad (4)$$

If the polarization of the nucleon 1 outgoing in the scattering plane is detected, the structure functions can in general be written as

$$f_{\lambda\lambda'} = h^u_{\lambda\lambda'} + \hat{\boldsymbol{s}} \cdot \boldsymbol{h}_{\lambda\lambda'},$$
$$f'_{\lambda\lambda'} = h'^u_{\lambda\lambda'} + \hat{\boldsymbol{s}} \cdot \boldsymbol{h}'_{\lambda\lambda'} \qquad (5)$$
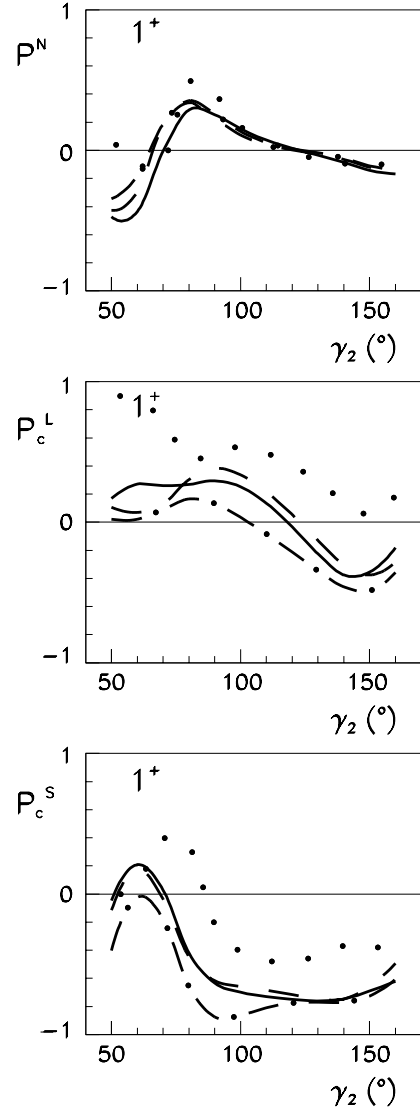
where $\hat{\boldsymbol{s}}$ is the unit vector in the spin direction of the recoil nucleon. Thus, when the polarization of the outgoing nucleon is considered, 16 structure functions appear: 4 spin
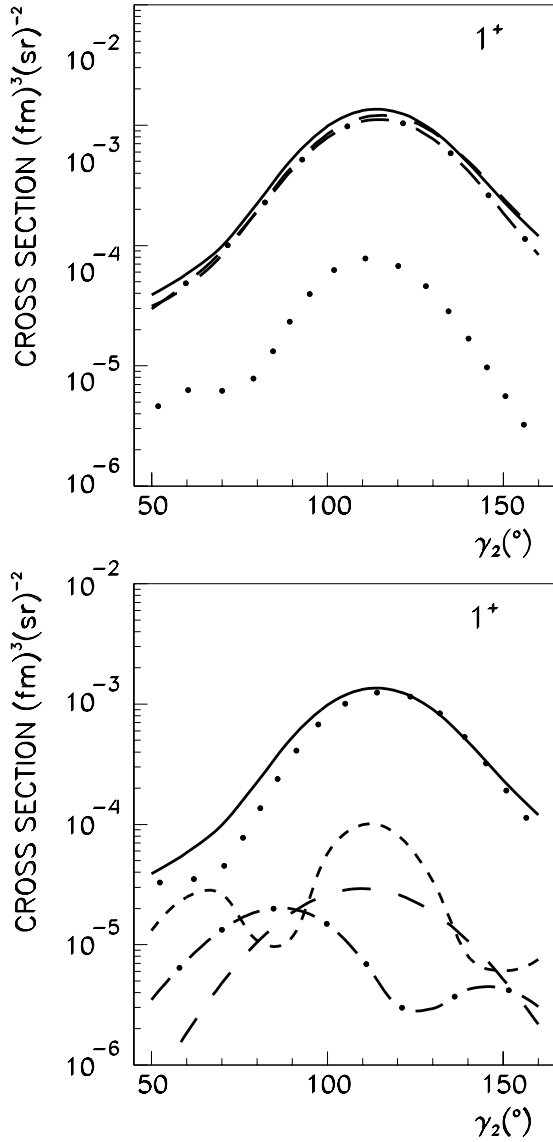
Fig. 3. The differential cross-section of the $^{16}O(\gamma, np)^{14}N_{g.s.}$ reaction as a function of the scattering angle γ_2 of the outgoing proton in a coplanar kinematics at $E_\gamma = 120$ MeV, with an outgoing-neutron energy $T_n = 45$ MeV and $\gamma_1 = 45°$. The optical potential is taken from ref. [17]. In the upper panel the same line convention as in fig. 1 is used. In the lower panel separate contributions of different partial waves of relative motion are drawn: the dotted line is for $^3S_1$, the dot-dashed line is for $^1P_1$, the long-dashed line gives the $^3D_1$ component already present in the uncorrelated wave function and the short-dashed line gives the $^3D_1^T$ component due to tensor correlations. The solid line is the same as in the upper panel.

Fig. 4. The polarization observables P^N, P_c^L, and P_c^S for the same reaction and in the same conditions and kinematics as in fig. 3. Line convention as in the upper panel of fig. 3.

independent, $h_{\lambda\lambda'}^u$ and $h_{\lambda\lambda'}'^u$, and 12 spin dependent, $h_{\lambda\lambda'}^k$ and $h_{\lambda\lambda'}'^k$, 4 for each one of the 3 components of $\boldsymbol{h}_{\lambda\lambda'}$ and $\boldsymbol{h}_{\lambda\lambda'}'$.

The explicit expressions of these structure functions in terms of the components of the hadron tensor $W_{\alpha\alpha'}^{\mu\nu}$, where α and α' are the eigenvalues of the spin of the nucleon whose polarization is considered, can be easily obtained from eq. (4), by simply substituting the quantities $W^{\mu\nu}$,

wherever they appear, with the following expressions [24]:

$$
\begin{aligned}
W_{++}^{\mu\nu} + W_{--}^{\mu\nu} & \quad \text{for} \quad k = u, \\
W_{+-}^{\mu\nu} + W_{-+}^{\mu\nu} & \quad \text{for} \quad k = x, \\
i(W_{+-}^{\mu\nu} - W_{-+}^{\mu\nu}) & \quad \text{for} \quad k = y, \\
W_{++}^{\mu\nu} - W_{--}^{\mu\nu} & \quad \text{for} \quad k = z.
\end{aligned}
\tag{6}
$$

Note that in ref. [24] there is a misprint in the case $k = y$.

Usually, the quantities $\boldsymbol{h}_{\lambda\lambda'}$ and $\boldsymbol{h}_{\lambda\lambda'}'$ are projected onto the basis of unit vectors given by $\hat{\boldsymbol{L}}$ (parallel to $\boldsymbol{p}_1'$), $\hat{\boldsymbol{N}}$ (in the direction of $\boldsymbol{q} \times \boldsymbol{p}_1'$) and $\hat{\boldsymbol{S}} = \hat{\boldsymbol{N}} \times \hat{\boldsymbol{L}}$, and the structure functions are thus given for the components $k = N, L, S$.

When the outgoing-nucleon polarization is not detected, the cross-section is summed over the spin quantum numbers of the outgoing nucleon and the spin independent
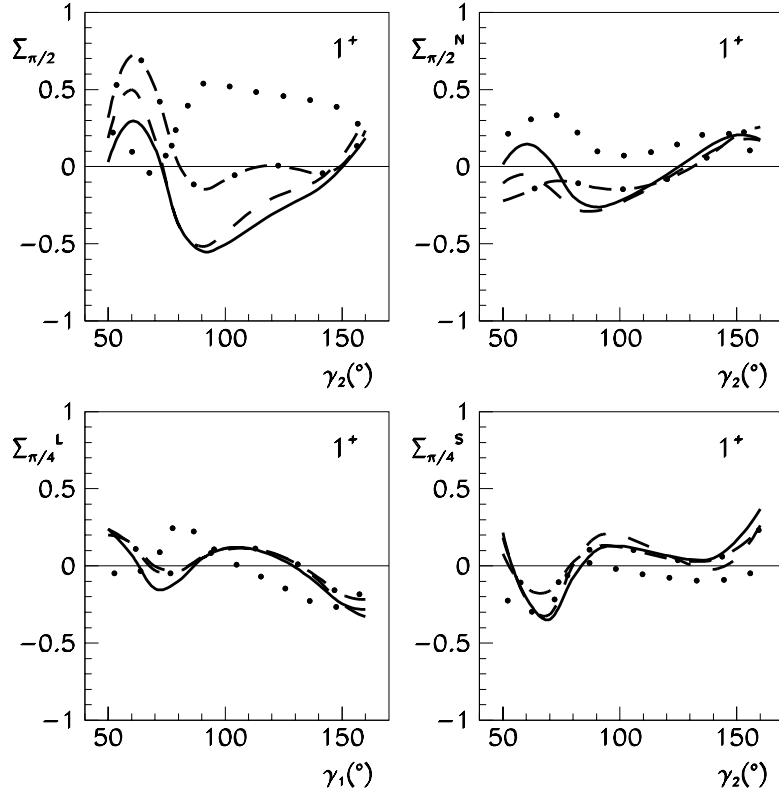
Fig. 5. The polarization observables $\Sigma_{\pi/2}$ $\Sigma_{\pi/2}^N$, $\Sigma_{\pi/4}^L$, and $\Sigma_{\pi/4}^S$ for the same reaction, in the same conditions and kinematics and with the same line convention as in the upper panel of fig. 3.

structure functions $h_{\lambda\lambda'}^u$ go over to the structure functions $f_{\lambda\lambda'}$ of the unpolarized case [2,24]. Thus, in this case only four structure functions are obtained, $f_{\lambda\lambda'} = 2h_{\lambda\lambda'}^u$, and four independent quantities can be measured: the unpolarized cross-section

$$\sigma_0 = \frac{2\pi^2\alpha}{E_\gamma} K \, 2h_{11}^u, \tag{7}$$

the circular asymmetry

$$A_c = \frac{\sigma(+) - \sigma(-)}{\sigma(+) + \sigma(-)} = \frac{h_{11}'^u}{h_{11}^u}, \tag{8}$$

where $\sigma(+)$ and $\sigma(-)$ are the cross-sections for a circularly polarized photon and $\Pi_t = 0$, and the two independent linear asymmetries

$$\Sigma_{\frac{\pi}{2}} = \frac{\sigma(0) - \sigma(\frac{\pi}{2})}{\sigma(0) + \sigma(\frac{\pi}{2})} = -\frac{h_{1-1}^u}{h_{11}^u} \tag{9}$$

and

$$\Sigma_{\frac{\pi}{4}} = \frac{\sigma(\frac{\pi}{4}) - \sigma(-\frac{\pi}{4})}{\sigma(\frac{\pi}{4}) + \sigma(-\frac{\pi}{4})} = \frac{\bar{h}_{1-1}^u}{h_{11}^u}, \tag{10}$$

where $\sigma(0)$, $\sigma(\frac{\pi}{2})$ and $\sigma(\frac{\pi}{4})$ are the cross-sections for a linearly polarized photon in the directions $\phi_\gamma = 0, \frac{\pi}{2}$, and $\frac{\pi}{4}$, respectively, and $\Pi_c = 0$.

When the polarization of the outgoing nucleon is detected, the 12 new structure functions $h_{\lambda\lambda'}^k$ and 12 corresponding polarization observables, 4 for each direction N,

L, and S, are produced. For an unpolarized photon, we have the components of the polarization

$$P^k = \frac{\sigma(+1) - \sigma(-1)}{\sigma(+1) + \sigma(-1)} = \frac{h_{11}^k}{h_{11}^u}, \tag{11}$$

where $\sigma(+1)$ $(\sigma(-1))$ are the cross-sections with a nucleon polarized parallel (antiparallel) to the component $\hat{s}^k$ of the spin direction given in eq. (5).
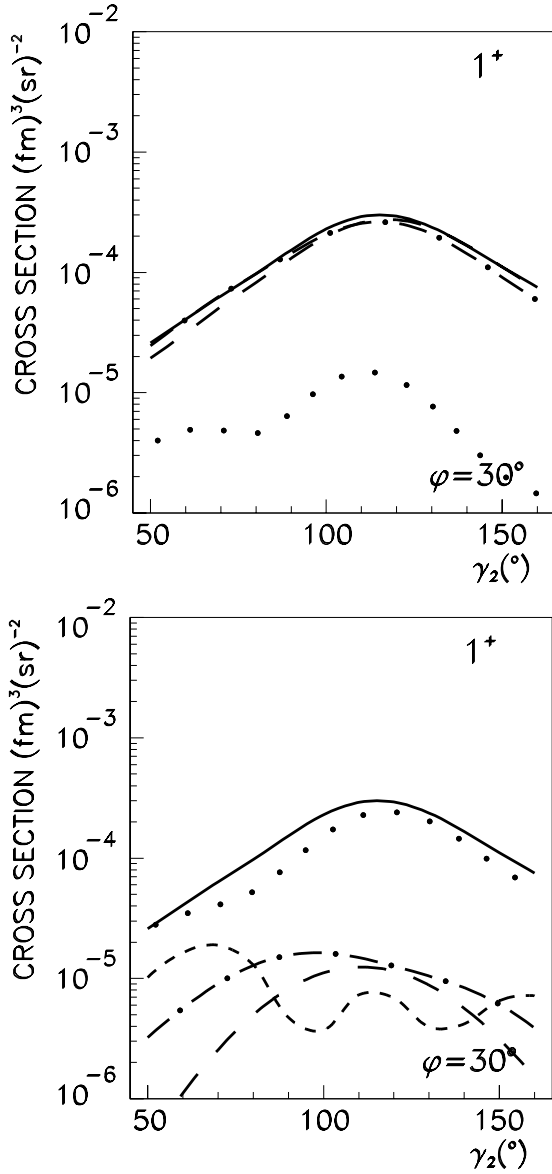
If the photon is circularly polarized and $\Pi_t = 0$, we have the components of the polarization transfer coefficient

$$P_c^k = \frac{\sigma(+,+1) - \sigma(+,-1) - \sigma(-,+1) + \sigma(-,-1)}{\sigma(+,+1) + \sigma(+,-1) + \sigma(-,+1) + \sigma(-,-1)} = \frac{h_{11}'^k}{h_{11}^u}, \tag{12}$$

where, here and in the following, the first argument in σ refers to the photon polarization and the second to the nucleon polarization in the direction $\hat{s}^k$.

For a linearly polarized photon and $\Pi_c = 0$, we have the components of the two polarization asymmetries

$$\Sigma_{\frac{\pi}{2}}^k = \frac{\sigma(0,+1) - \sigma(0,-1) - \sigma(\frac{\pi}{2},+1) + \sigma(\frac{\pi}{2},-1)}{\sigma(0,+1) + \sigma(0,-1) + \sigma(\frac{\pi}{2},+1) + \sigma(\frac{\pi}{2},-1)} = -\frac{h_{1-1}^k}{h_{11}^u} \tag{13}$$

Table 1. Properties of the structure functions and polarization observables.

		Survives in plane	Survives in PW
h_{11}^u	σ_0	yes	yes
$h_{11}'^u$	A_c	no	no
h_{1-1}^u	$\Sigma_{\frac{\pi}{2}}$	yes	yes
$\bar{h}_{1-1}^u$	$\Sigma_{\frac{\pi}{4}}$	no	yes
h_{11}^N	P^N	yes	no
$h_{11}'^N$	P_c^N	no	yes
h_{1-1}^N	$\Sigma_{\frac{\pi}{2}}^N$	yes	no
$\bar{h}_{1-1}^N$	$\Sigma_{\frac{\pi}{4}}^N$	no	no
$h_{11}^{L,S}$	$P^{L,S}$	no	no
$h_{11}'^{L,S}$	$P_c^{L,S}$	yes	yes
$h_{1-1}^{L,S}$	$\Sigma_{\frac{\pi}{2}}^{L,S}$	no	no
$\bar{h}_{1-1}^{L,S}$	$\Sigma_{\frac{\pi}{4}}^{L,S}$	yes	no

Fig. 6. The differential cross-section of the $^{16}\mathrm{O}(\gamma, np)^{14}\mathrm{N}_{\mathrm{g.s.}}$ reaction as a function of the scattering angle γ_2 of the outgoing proton in an out-of-plane kinematics at $E_\gamma = 120$ MeV, with $T_n = 45$ MeV, $\gamma_1 = 45°$ and the azimuthal angle of the outgoing proton $\phi = 30°$. The optical potential is taken from ref. [17]. Line convention in the upper and lower panels as in fig. 3.

and

$$\Sigma_{\frac{\pi}{4}}^k = \frac{\sigma(\frac{\pi}{4},+1) - \sigma(\frac{\pi}{4},-1) - \sigma(-\frac{\pi}{4},+1) + \sigma(-\frac{\pi}{4},-1)}{\sigma(\frac{\pi}{4},+1) + \sigma(\frac{\pi}{4},-1) + \sigma(-\frac{\pi}{4},+1) + \sigma(-\frac{\pi}{4},-1)} = \frac{\bar{h}_{1-1}^k}{h_{11}^u}, \qquad (14)$$

where the first argument in σ refers to the value of the angle ϕ_γ.

In the case of a coplanar kinematics, where both the emitted nucleons and the photon lie in the same plane, owing to parity conservation combined with the general properties of the hadron tensor, several structure functions vanish and only 8 of them survive: h_{11}^u, h_{11}^N, h_{1-1}^u, h_{1-1}^N, $h_{11}'^{L,S}$ and $\bar{h}_{1-1}^{L,S}$ and thus the quantities σ_0, P^N, $\Sigma_{\frac{\pi}{2}}$, $\Sigma_{\frac{\pi}{2}}^N$, $P_c^{L,S}$, and $\Sigma_{\frac{\pi}{4}}^{L,S}$ can be measured. This result can be derived along the same lines as the one obtained in ref. [24] in the more general case of the $(\vec{e}, e'\vec{N}N)$ reaction, and is similar to the result obtained for the $(\vec{\gamma}, \vec{N})$ reaction [2].

When the nucleon spin is not detected, in coplanar kinematics the only dynamical variable with a nonvanishing component in the y direction is the pseudovector $\boldsymbol{q} \times \boldsymbol{p}_1'$. As no pseudovectors are available with a component along x, the matrix elements of the hadron tensor W^{xy} and W^{yx} must vanish. Therefore, $h_{11}'^u = \bar{h}_{1-1}^u = 0$ and, consequently, $A_c = \Sigma_{\frac{\pi}{4}} = 0$, and only $\Sigma_{\frac{\pi}{2}}$ survives.

When the nucleon spin is detected, owing to the properties of the spin-$\frac{1}{2}$ matrix, only a linear dependence of the structure functions on the spin is allowed (see eq. (5)). As the spin is a pseudovector and in order to fulfill parity conservation, it must be coupled in the hadron tensor with the only available pseudovector independent of the spin, i.e. with $\boldsymbol{q} \times \boldsymbol{p}_1'$, which in coplanar kinematics is directed along y. Therefore, we have: $W^{xx} = 0$, W^{yy} dependent on s^N, and W^{xy} independent of s^N. As a consequence, one has: $h_{11}'^N = \bar{h}_{1-1}^N = h_{11}^{L,S} = h_{1-1}^{L,S} = 0$. Thus, $P^{L,S}$, $\Sigma_{\frac{\pi}{2}}^{L,S}$, P_c^N and $\Sigma_{\frac{\pi}{4}}^N$ vanish and only P^N, $\Sigma_{\frac{\pi}{2}}^N$, $P_c^{L,S}$ and $\Sigma_{\frac{\pi}{4}}^{L,S}$ survive.

The behaviour of the hadron tensor under time reversal and parity transformation has the property [24,25]

$$W^{\mu\nu}(\boldsymbol{s}, (-)) = W^{\nu\mu}(-\boldsymbol{s}, (+)), \qquad (15)$$
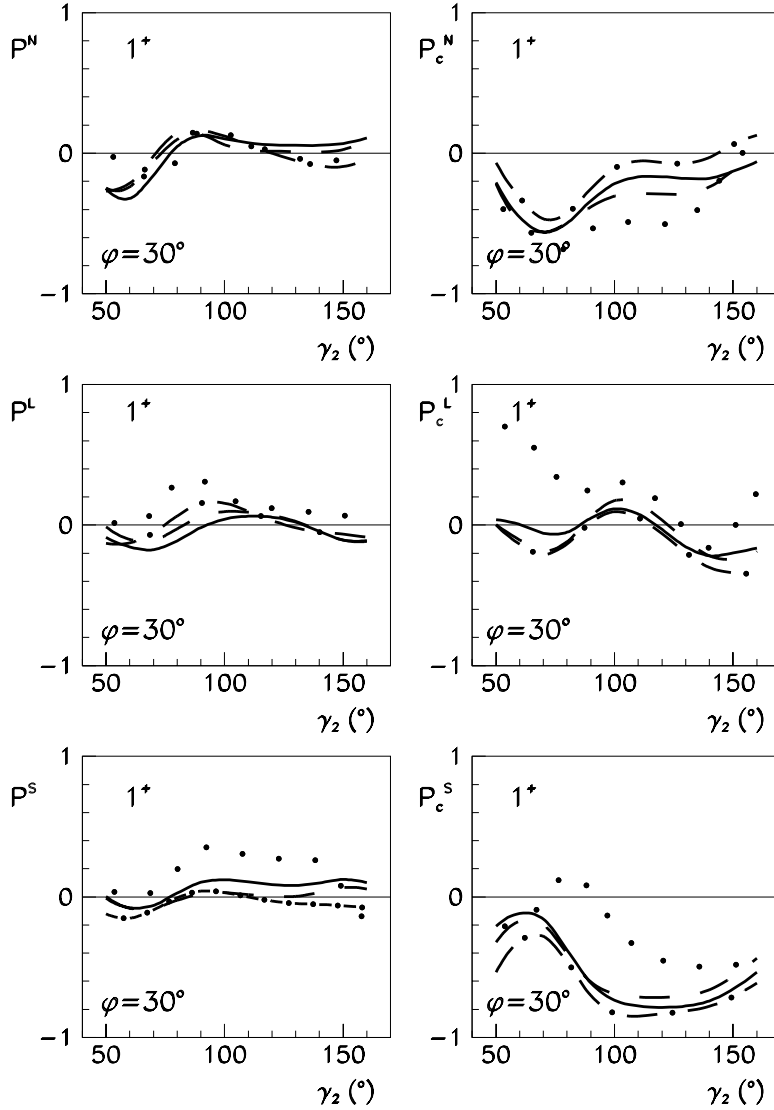
Fig. 7. The polarization observables P^N, P_c^N, P^L, P_c^L, P^S, and P_c^S for the same reaction and in the same conditions and kinematics as in fig. 6. Line convention as in the upper panel of fig. 3.

where s is the spin vector in the ejectile rest frame, and the dependence on the final-state boundary condition for incoming $(-)$ and outgoing $(+)$ scattered waves is shown. For nucleon knockout, the $(-)$ condition is appropriate. When the boundary conditions can be ignored, as in the plane-wave (PW) approximation, eq. (15) states that the symmetric part of $W^{\mu\nu}$ is independent of s and the antisymmetric part is proportional to s. Therefore, when the hadron tensor is spin independent its antisymmetric part vanishes, while its symmetric part vanishes when it is spin dependent. Thus, in PW only h_{11}^u, h_{1-1}^u, $\bar{h}_{1-1}^u$, and $h_{11}'^{N,L,S}$ survive and therefore σ_0, $\Sigma_{\frac{\pi}{2}}$, $\Sigma_{\frac{\pi}{4}}$, and $P_c^{N,L,S}$, while $A_c = P^{N,L,S} = \Sigma_{\frac{\pi}{2}}^{N,L,S} = \Sigma_{\frac{\pi}{4}}^{N,L,S} = 0$.

If both coplanar kinematics and the PW approximation are considered, only σ_0, $\Sigma_{\frac{\pi}{2}}$ and $P_c^{L,S}$ survive. The results are summarized in table 1.

3 The ^{16}O$(\vec{\gamma}, \vec{n}p)^{14}$N reaction

In this section numerical results are presented for the ^{16}O$(\gamma, np)^{14}$N reaction. Calculations have been performed within the theoretical framework of ref. [16]. In this model it is possible to consider transitions to different low-lying discrete states of the residual nucleus, that are expected to be strongly populated by direct knockout. Here, we present numerical examples for the transition to the 1^+ ground state of ^{14}N, with $T = 0$. This is the first state that can be experimentally separated with an energy resolution of a few MeV and is therefore of particular interest.

The results are very sensitive to the theoretical treatment of the two-nucleon overlap between the ground state of the target and the final state of the residual nucleus. An example is shown in fig. 1, where the calculated differential cross-sections of the ^{16}O(γ, np) reaction are displayed in a coplanar and symmetrical kinematics at the incident
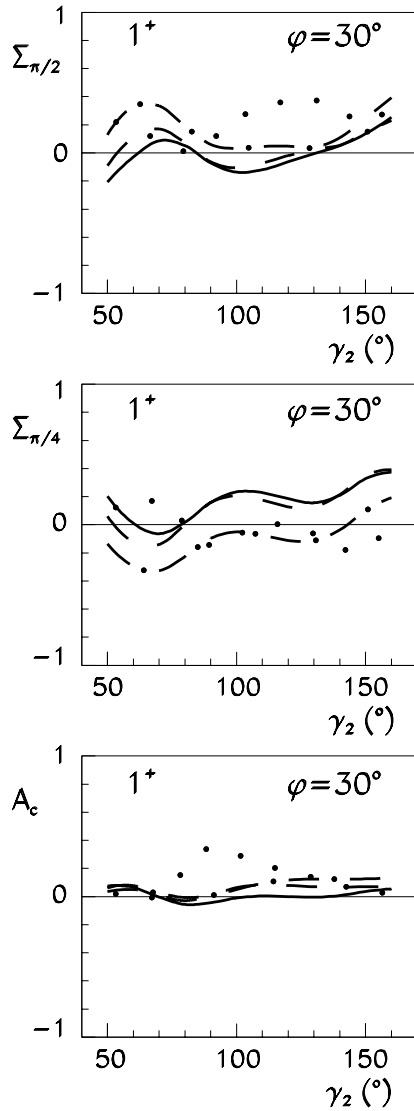
Fig. 8. The polarization observables $\Sigma_{\pi/2}$, $\Sigma_{\pi/4}$, and $A_{\rm c}$ for the same reaction and in the same conditions and kinematics as in fig. 6. Line convention as in the upper panel of fig. 3.

photon energies of $E_\gamma = 100$ MeV and 400 MeV. In this kinematics the two nucleons are emitted in the scattering plane at equal energies and equal but opposite angles with respect to the beam direction. Then, for a fixed value of E_γ and changing the value of the scattering angle it is possible to explore all values of the recoil ($p_{\rm r}$) or missing momentum ($p_{2\rm m}$) distribution. One has

$$\boldsymbol{p}_{2\rm m} = \boldsymbol{p}_{\rm r} = \boldsymbol{q} - \boldsymbol{p}'_1 - \boldsymbol{p}'_2, \qquad (16)$$

where $\boldsymbol{q}$, $\boldsymbol{p}'_1$, and $\boldsymbol{p}'_2$ are the momenta of the incident photon and of the two outgoing nucleons, respectively.

If relative and c.m. motions are factorized and final-state interactions are neglected [1], $\boldsymbol{p}_{\rm r}$ is opposite to the total momentum $\boldsymbol{P}$ of the nucleon pair in the target. Thus, the shape of the momentum distribution is driven by the c.m. orbital angular momentum of the knocked-out pair. As this feature is not spoiled in an unfactorized approach,

the symmetrical kinematics here considered is well suited to give information on the motion of the pair in different c.m. angular momentum states.

Calculations have been performed within the direct knockout framework of refs. [16,9], where the final-state wave function includes the interaction of each one of the two outgoing nucleons with the residual nucleus by means of a phenomenological optical potential. The nuclear current is the sum of a one-body part, including convective and spin currents, and of a two-body part, including terms corresponding to the lowest order diagrams with one-pion exchange, namely seagull, pion-in-flight and those with intermediate Δ isobar configurations.

The results given by two different treatments of the two-nucleon overlap are compared in the upper and lower panels of fig. 1. The cross-sections displayed in the upper panels are obtained with the overlap integral used in [16] for the ^{16}O$(e, e'np)^{14}$N reaction. It includes the effects of short-range as well as tensor correlations, which are calculated within the framework of the coupled cluster method and with a correlation operator restricted to $1p$-$1h$ and $2p$-$2h$ excitations. The Argonne V14 potential [26] is employed as a model for a realistic nucleon-nucleon interaction. The explicit expression of the two-nucleon overlap is given by an expansion over relative and c.m. wave functions. The expansion coefficients, accounting for the global or long-range structure of the specific nuclear states, are determined from a configuration mixing calculation of the two-hole states in ^{16}O, which can be coupled to the angular momentum and parity of the requested final state and are renormalized to account for the spectroscopic factors of the s.p. states. This is the best model which can be applied at present, as it contains all the complications of a many-body calculation and the effects of a realistic interaction.

The results in the lower panels are calculated with the simpler prescription used in ref. [9], *i.e.* by the product of the pair function of the shell model, described for the 1^+ ground state of ^{14}N as a pure $(p_{1/2})^{-2}$ hole, and of a Jastrow-type central and state independent correlation function [27]. With this simpler prescription the contribution of the one-body currents and thus of correlations is much lower than with the more refined model, where also tensor correlations are included. In both cases, however, and for both values of the photon energy, the calculated cross-sections are dominated by two-body currents, *i.e.* by the seagull current at 100 MeV and by the Δ current at 400 MeV. The differences between the results shown in the upper and lower panels of the figure are anyhow large. They are in particular due to the presence in the model of ref. [16], together with the $(p_{1/2})^{-2}$ component, with a strength 0.60, of an interference component $(p_{1/2}p_{3/2})^{-1}$ equal to -0.45 [16]. These differences, which are due only to the treatment of the two-nucleon overlap, clearly show that the shape and the size of the cross-section are very sensitive to this treatment and that an accurate description of both aspects related to nuclear structure and correlations is needed to produce reliable numerical predictions. This result, that is well established
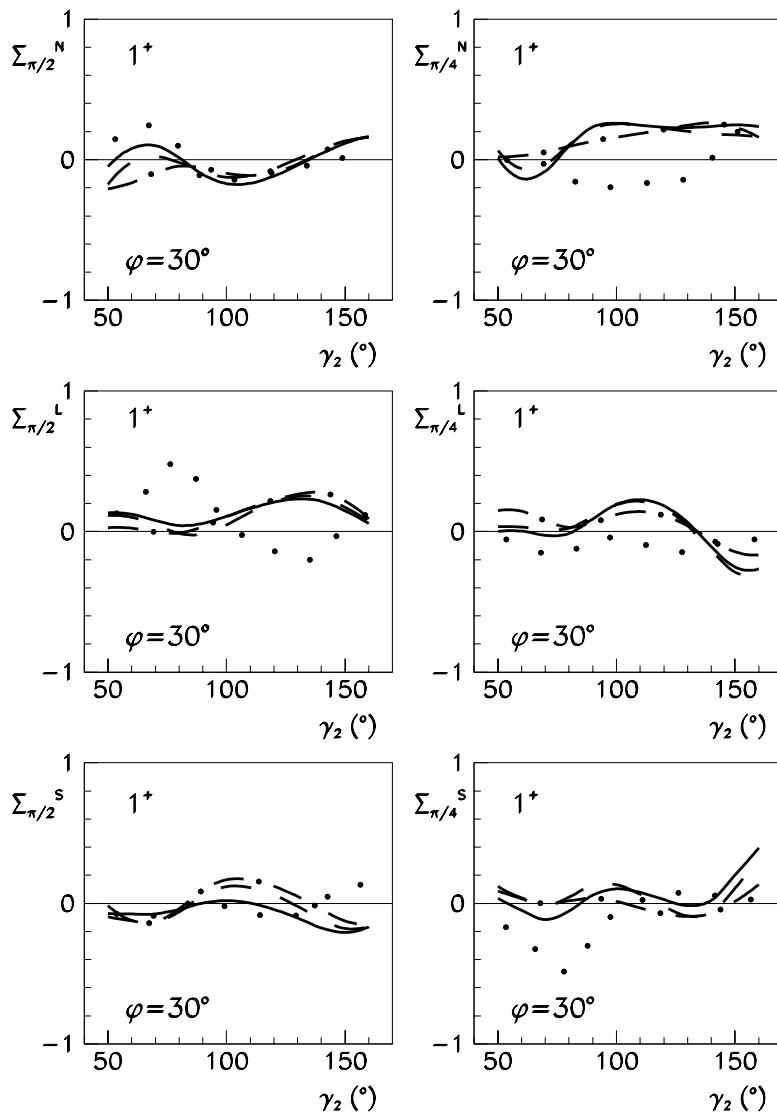
Fig. 9. The polarization observables $\Sigma_{\pi/2}^N$, $\Sigma_{\pi/4}^N$, $\Sigma_{\pi/2}^L$, $\Sigma_{\pi/4}^L$, $\Sigma_{\pi/2}^S$, and $\Sigma_{\pi/4}^S$ for the same reaction and in the same conditions and kinematics as in fig. 6. Line convention as in the upper panel of fig. 3.

for $(e, e'NN)$ reactions [11–14], is therefore confirmed also for two-nucleon knockout induced by real photons.

The linear asymmetry $\Sigma_{\frac{\pi}{2}}$, calculated with the two different prescriptions for the overlap integral and in the same conditions and kinematics as in fig. 1, is shown in fig. 2. Large differences are given also in this case by the two models, both at $E_\gamma = 100$ and 400 MeV. The contribution of the one-body current is generally small. This confirms that even when two-body currents are dominant the results can be very sensitive to nuclear structure and correlation effects. Moreover, as it was already observed in previous investigations [9,10], the asymmetry appears particularly affected by the different terms of the two-body current and by their interference, in particular by the interference between the pion-in-flight and seagull currents. This contribution is dominant on the asymmetry at $E_\gamma = 100$ MeV, while the role of pion-in-flight on the cross-section is generally small. At $E_\gamma = 400$ MeV the Δ

current gives the main contribution, which, however, is not as dominant as in the cross-section. Nonnegligible effects are given also by the other components of the two-body current.

For the following calculations we have chosen a coplanar kinematics at $E_\gamma = 120$ MeV. At this value of the photon energy, far from the peak of the Δ resonance, the contribution of the two-body Δ current, that is an important but difficult ingredient [28] of the theoretical model, is drastically reduced. However, the photon energy is large enough to obtain outgoing nucleons with a reduced final-state interaction. The contribution of meson exchange currents cannot be eliminated and the chosen energy is a compromise between the different contributions. The energy and the scattering angle of the outgoing neutron are fixed at 45 MeV and 45°, respectively. This value of the scattering angle is taken in order to minimise the mutual interaction between the outgoing nucleons. Different values
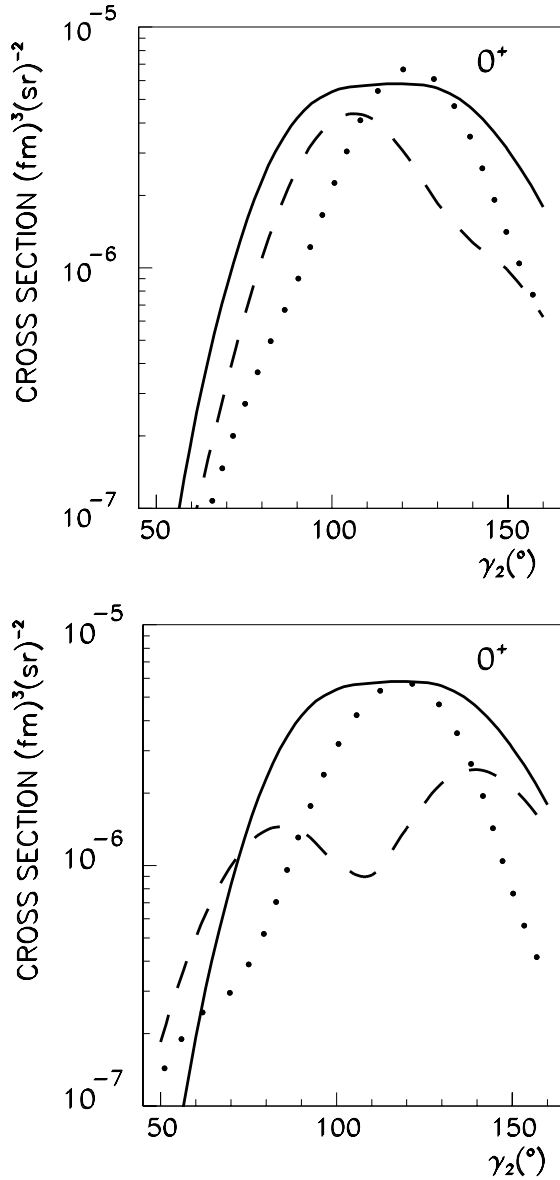
Fig. 10. The differential cross-section of the $^{16}O(\gamma, pp)^{14}C_{g.s.}$ reaction as a function of the scattering angle γ_2 in the same coplanar kinematics as in fig. 3. The defect functions for the Bonn-A potential and the optical potential of ref. [17] are used. The solid line gives the sum of the one-body and the two-body Δ current. In the upper panel the separate contributions given by the one-body currents (dotted line) and by the Δ current (dashed line) are drawn. In the lower panel separate contributions of different partial waves of relative motion are drawn: the dotted line is for $^1S_0$, the dashed line is for $^3P_1$.

of the recoil momentum can be obtained by varying the scattering angle of the outgoing proton. This kinematics appears within reach of available experimental facilities.

The calculated differential cross-section is displayed in fig. 3. In the upper panel the results given by the one-body current and by the addition of the different terms of the two-body current are shown. At the considered value of the photon energy the pion seagull current gives the
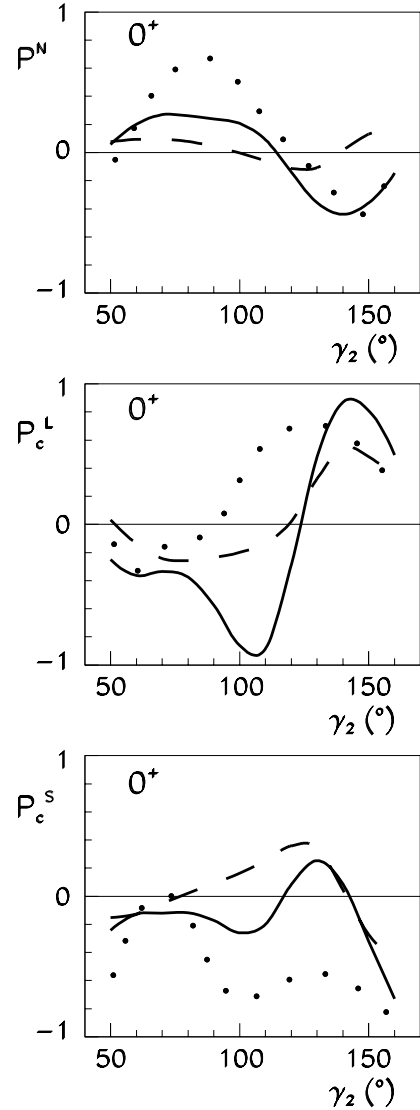
Fig. 11. The polarization observables P^N, P_c^L, and P_c^S for the same reaction and in the same conditions and kinematics as in fig. 10. Line convention as in the upper panel of fig. 10.

dominant contribution to the cross-section. Only a minor role is played by the one-body current and by the pion-in flight and Δ currents. The shape of the angular distribution, however, is practically the same as the one given by the one-body current.

In the considered kinematics and in the calculated angular range, the recoil momentum varies between $\simeq 90$ and 290 MeV/c, on both sides of the distribution. The shape of the distribution is driven by the c.m. orbital angular momentum L of the knocked-out pair. In our model the two-nucleon overlap function contains different components of relative and c.m. motion [16]. For the transition to the 1^+ ground state the relative waves are: $^3S_1$ (the notation $^{2S+1}l_j$, for $l = S, P, D$, is used here for the relative states), combined with a c.m. $L = 0$ and $L = 2$, $^1P_1$, combined with $L = 1$, and $^3D_1$. For this relative wave we have separated the component already present in
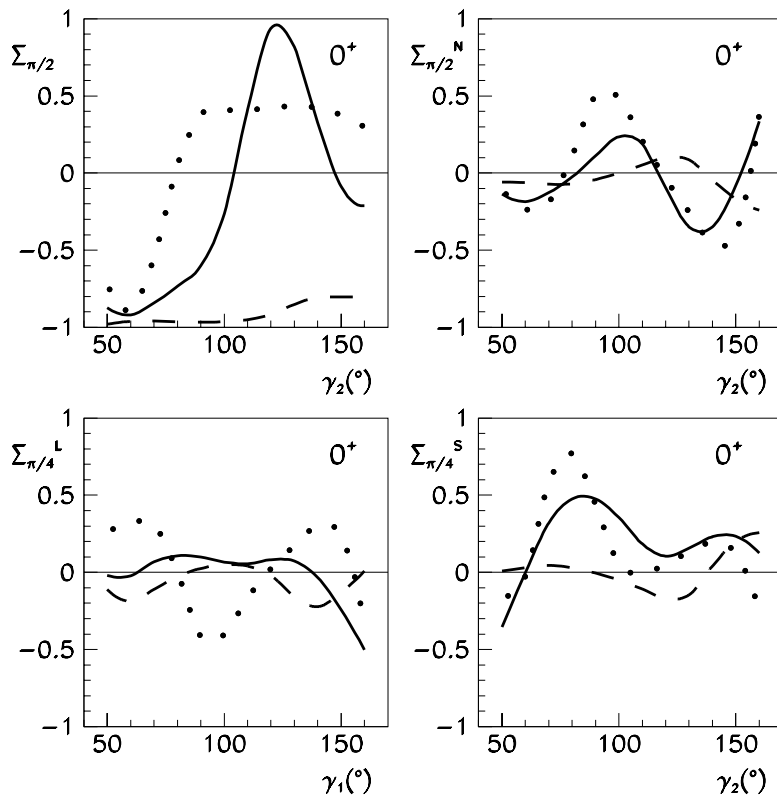
Fig. 12. The polarization observables $\Sigma_{\pi/2}$ $\Sigma_{\pi/2}^N$, $\Sigma_{\pi/4}^L$, and $\Sigma_{\pi/4}^S$ for the same reaction, in the same conditions and kinematics and with the same line convention as in the upper panel of fig. 10.

the uncorrelated wave function, which is combined with $L = 0$, and the one produced by tensor correlations and not present in the uncorrelated wave function, which is combined with $L = 0$ and $L = 2$. As in ref. [16] we call these two terms $^3D_1$ and $^3D_1^{\mathrm{T}}$, respectively. The contribution of $^3D_1^{\mathrm{T}}$ emphasizes the role played in the calculations by tensor correlations, which are anyhow present also in the other components.

The separate contributions of the different waves of relative motion are shown in the lower panel of fig. 3. The shape of the different curves is determined by the corresponding values of L. The shape of the final cross-section is driven by the component which gives the major contribution, *i.e.* by $^3S_1$ in the considered case. Only small effects are given by the other partial waves. The component $^3D_1^{\mathrm{T}}$, in particular its part with $L = 2$, is nonnegligible at low values of the scattering angle, which correspond to larger values of the momentum. The cross-section is thus basically a combination of states with $L = 0$ and $L = 2$. The contribution of the state with $L = 1$ for $^1P_1$ is very small. The main role is played by the state with $L = 0$ for $^3S_1$, which gives the *s*-wave shape in the figure. The contribution of states with $L = 2$ for $^3S_1$ and $^3D_1^{\mathrm{T}}$ becomes important at large values of the recoil momentum, where the contribution of the state with $L = 0$ becomes much lower.

It has been shown in sect. 2 that when the incident photon is polarized and/or the polarization of the outgoing nucleon is detected, 7 polarization observables survive

in coplanar kinematics: the asymmetry $\Sigma_{\frac{\pi}{2}}$, that can be measured in a reaction with a linearly polarized photon and where the nucleon recoil polarization is not detected, the component P^N of the outgoing-nucleon polarization, that can be measured in a reaction with an unpolarized incident photon, the components $P_{\mathrm{c}}^{L,S}$ of the polarization transfer coefficient, that can be measured in a reaction with a circularly polarized photon, and the components $\Sigma_{\frac{\pi}{2}}^N$ and $\Sigma_{\frac{\pi}{4}}^{L,S}$ of the polarization asymmetries, that can be measured in a reaction with a linearly polarized incident photon.

The polarization observables calculated with our model and in the coplanar kinematics of fig. 3 are shown in figs. 4 and 5. The results indicate that all the observables are sizable. They are sensitive to all the different terms of the nuclear current and also to their interference. The main contribution is generally given by the seagull current, which, however, is not as dominant as in the cross-section. A large effect is given by the interference between the seagull and pion-in-flight terms, in particular for the asymmetry $\Sigma_{\frac{\pi}{2}}$, where this effect gives the main contribution. The role of the one-body current is not very important in general, but it can be meaningful in particular situations, for instance on P^N. At the considered value of the photon energy, $E_\gamma = 120$ MeV, a small although nonnegligible effect is generally given by the Δ current.

We note that $\Sigma_{\frac{\pi}{2}}^N$ and $\Sigma_{\frac{\pi}{4}}^{L,S}$ vanish in the PW approximation, when final-state interactions (FSI) are neglected.
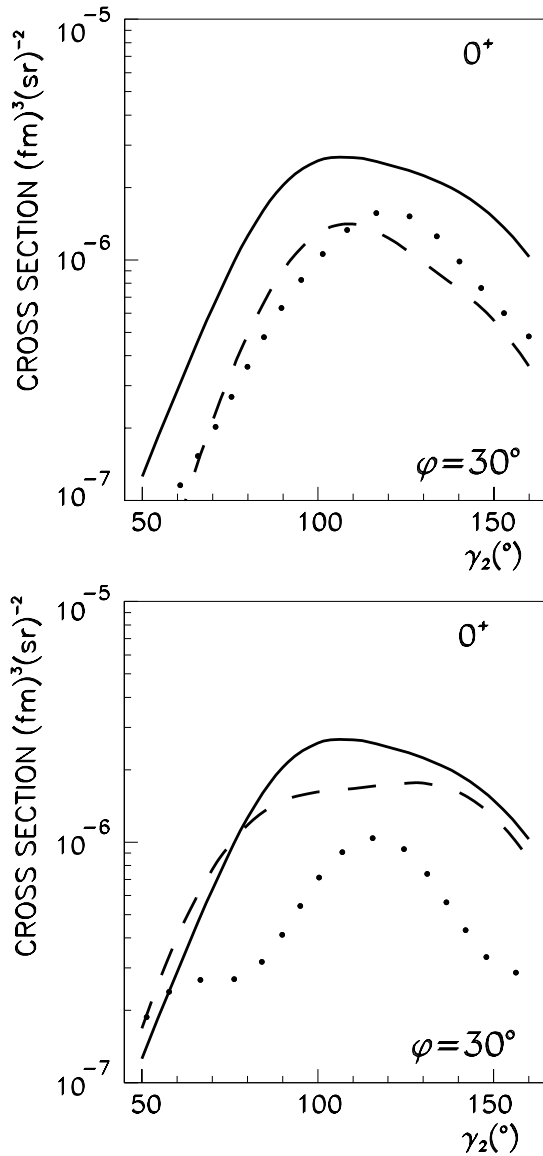
Fig. 13. The differential cross-section of the $^{16}\text{O}(\gamma, pp)^{14}\text{C}_{\text{g.s.}}$ reaction as a function of the scattering angle γ_2 in the same out-of-plane kinematics as in fig. 6. Defect functions, optical potential and line convention as in fig. 10.

Indeed in fig. 5 these quantities turn out to be smaller than the other observables which are present also in PW. Since they are produced by FSI, one might expect that they are sensitive to their treatment.

The results depend on kinematics and on the final state that is considered. The numerical example in figs. 3-5 indicates that cross-sections and polarization observables show a different sensitivity to the different terms of the nuclear current. This can be understood if one considers that different structure functions contribute to the different quantities. Moreover, since the polarization observables can be expressed in terms of ratios between the various structure functions and h_{11}^u, that gives the unpolarized cross-section, one can expect that they are able to emphasize specific effects that can be smoothed out in the

cross-section. Thus, a combined experimental determination of cross-sections and polarization observables would give a complete information on the reaction process. It would impose constraints to the different theoretical ingredients and result in a stringent test of theoretical models. In figs. 3-5 we have shown the sensitivity to the different terms of the nuclear current. In figs. 1 and 2, in different kinematics, it has been shown that the cross-section and the photon asymmetry $\Sigma_{\frac{\pi}{2}}$ exhibit a strong and different sensitivity to the theoretical treatment of the two-nucleon overlap.

A complete study of all the 16 observables defined in sect. 2 requires an out-of-plane kinematics. A numerical example is shown in figs. 6-9 in a situation where the azimuthal angle ϕ of the outgoing nucleon whose polarization is not considered (the proton in our case) is $30°$. The other kinematical variables are taken as in the coplanar kinematics of fig. 3.

The differential cross-section in fig. 6 confirms the dominant role of the seagull current and of the $^3S_1$ component. The size, however, is an order of magnitude lower than in the peak region of the coplanar kinematics, while the shape indicates a less pronounced peak and a larger contribution of the components with $L = 2$. The main reason of the differences can be attributed to a kinematic effect. Different values of the recoil momentum are obtained for the same angle γ_2 in the two kinematics. When the outgoing nucleon is taken out of the plane, values lower than 160 MeV/c are forbidden and the region between 90 and 160 MeV/c, where the cross-section in the coplanar kinematics has the maximum, is cut. This explains the different size and shape of the results in figs. 3 and 6. This kinematic effect gives also the main difference between the calculated polarization observables which are present both in coplanar and out-of-plane kinematics. The other observables, which are nonvanishing only in out-of-plane kinematics, are sizable. In the considered situation the main contribution is generally given by the seagull current, but also the other terms, in particular the interference between seagull and pion-in-flight, can be meaningful in some observables.

4 The $^{16}\text{O}(\vec{\gamma}, \vec{p}p)^{14}\text{C}$ reaction

In this section numerical results are presented for the $^{16}\text{O}(\gamma, pp)^{14}\text{C}$ reaction. Calculations have been performed within the theoretical framework of ref. [15]. The model is basically the same used for the $^{16}\text{O}(\gamma, np)^{14}\text{N}$ reaction where the nuclear current is adapted to a pp pair. Thus, in the two-body current the charge-exchange terms vanish and only a part of the Δ current contributes. However, a different treatment of the two-nucleon overlap function is used, based on the results of the calculation of the two-proton spectral function of ^{16}O [29,15]. The two-nucleon overlaps for transitions to the lowest-lying discrete final states of the residual nucleus are obtained from a two-step procedure, where long-range and short-range correlations are treated in a separate but consistent way. The calculation of long-range correlations is performed in a
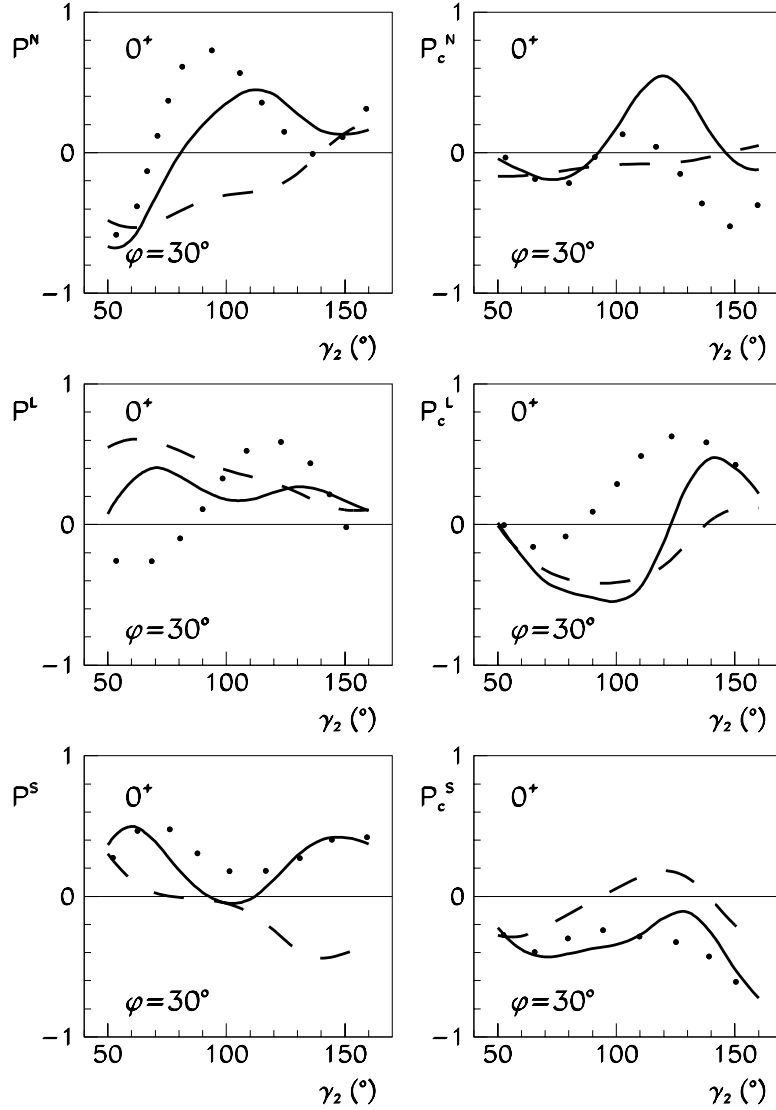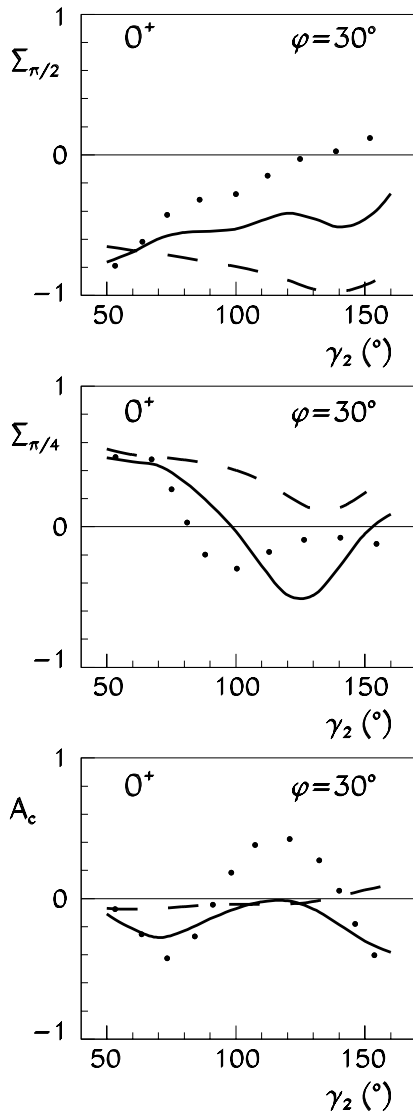
Fig. 14. The polarization observables P^N, P_{c}^N, P^L, P_{c}^L, P^S, and P_{c}^S for the same reaction and in the same conditions and kinematics as in fig. 13. Line convention as in the upper panel of fig. 10.

shell model space large enough to incorporate the corresponding collective features which influence the pair removal amplitudes. The single-particle propagators used for this dressed Random Phase Approximation description of the two-particle propagator also include the effect of both long-range and short-range correlations. In the second step that part of the pair removal amplitudes which describes the relative motion of the pair is supplemented by defect functions, accounting for SRC and obtained from the same G-matrix which is also used as the effective interaction in the RPA calculation. The explicit expression of the overlap function is given in terms of a sum of products of relative and c.m. wave functions. Different components contribute to different transitions. Here, we present numerical results for the transition to the 0^+ ground state of ^{14}C, where the components are: $^1S_0$, which is combined with $L = 0$, and $^3P_1$, which is combined with $L = 1$. The ground state has been already separated in recent

high-resolution experiments for the ^{16}O$(e, e'pp)^{14}$C reaction [11–14]. The experimental cross-sections are well reproduced by the results of our model and clear evidence for SRC has been obtained in the comparison. Thus, it seems interesting to investigate the same final state also for the (γ, pp) reaction.

The differential cross-section of the ^{16}O$(\gamma, pp)^{14}$C reaction, calculated in the same coplanar kinematics considered in sect. 3, is displayed in fig. 10. The shape of the distribution is determined by the combination of the two components with $L = 0$ and $L = 1$. It is clearly shown in the lower panel of the figure that $^1S_0$ with its s-wave c.m. component prevails for angles corresponding to low values of the recoil momentum, where the p-wave has the minimum, while the contribution of $^3P_1$ knockout becomes important al large values of p_{r}, where the s-wave decreases.

It was established in previous investigations that SRC and two-body current play a different role in different rel-

Fig. 15. The polarization observables $\Sigma_{\pi/2}$, $\Sigma_{\pi/4}$, and $A_{\rm c}$ for the same reaction and in the same conditions and kinematics as in fig. 13. Line convention as in the upper panel of fig. 10.

ative states [11,13,15,24]. While SRC are quite strong for the $^1S_0$ state and much weaker for the ^3P_j states, the contribution of the two-body Δ current is strongly reduced in $^1S_0$ pp knockout [9,30] and generally dominant in ^3P_j knockout. Therefore, $^1S_0$ pp knockout is generally dominated by the contribution of the one-body current, and thus by SRC, while ^3P_j pp knockout is generally dominated by the Δ current. The selectivity of the reaction to different states was exploited in $(e,e'pp)$, where it was possible to envisage situations where either contribution is dominant and can thus be disentangled. The result, however, depends on kinematics and on the reaction that is considered. Thus, it cannot be directly applied to (γ,pp) reactions, where only the transverse components of the nuclear current contribute and the longitudinal component, where the effects of SRC show up more strongly, is absent. On the other hand, in the considered kinematics, where $E_\gamma = 120$ MeV, the contribution of the Δ current

should not be emphasized, as it is also demonstrated by the results of sect. 3 for the (γ,np) reaction.

In the present calculation the Δ current gives indeed the major contribution to $^3P_1$ knockout, but a sizable effect is also given by its interference with the one-body current. The one-body current is dominant in $^1S_0$ knockout. In the region of the maximum, where $^3P_1$ has the minimum, the contribution of the Δ current is larger in $^1S_0$ than in $^3P_1$. This explains the result in the upper panel of fig. 10. Most of the contribution of the one-body current is given by $^1S_0$ knockout. This determines the s-wave shape of the angular distribution. The result for the Δ current is due to the combined effect of $^3P_1$, which gives the main contribution at large values of $p_{\rm r}$, and of $^1S_0$, which enhances the cross-section with the Δ current at low values of $p_{\rm r}$. In the final cross-section both processes due to SRC and to the two-body current are important: SRC are of particular relevance at larger values of γ_2 and the Δ at lower values of γ_2.

The polarization observables are displayed in figs. 11 and 12. All the calculated quantities are sizable. Both contributions of the one-body and of the two-body current are important, even though the relevance of the two reaction mechanisms can be different for different observables. For instance, $\Sigma_{\frac{\pi}{2}}^N$ is basically given by the one-body current, while for other observables the final result, given by the sum of the one-body and the two-body current, is very different from the two separate contributions. Thus, a combined measurement of cross-sections and polarization observables would be able to disentangle the two reaction processes and to test the ingredients and the approximations of a theoretical model.

The cross-section and the polarization observables calculated for the $^{16}O(\gamma,pp)^{14}C$ reaction in the out-of-plane kinematics with $\phi = 30°$ are given in figs. 13-16. In comparison with the result for the coplanar kinematics, the cross-section in fig. 13 shows the same kinematic effect found in the $^{16}O(\gamma,np)^{14}N$ reaction. Values of $p_{\rm r}$ between 90 and 160 MeV/c are forbidden, and the region that in the coplanar kinematics of fig. 10 corresponds to the maximum of $^1S_0$ and to the minimum of $^3P_1$ is cut. As a consequence, the contribution of $^3P_1$ is always larger than the one of $^1S_0$ all over the angular distribution. The size of the final cross-section is reduced in the region of the maximum and a different shape is obtained. The contributions of the one-body and of the two-body current displayed in the upper panel are of about the same size and add up in the final cross-section. All the polarization observables in figs. 14-16 are sizable. Also in this case both the one-body and the two-body current are important. In some observables either contribution prevails or appears even dominant in the calculation, but both reaction processes are in general important in the final result and their theoretical treatment can be tested in combined measurements of the different observables.

Also the polarization observables which vanish in PW are sizable. Their determination might be of particular interest for the study of FSI, and in particular of the correlations between the two outgoing particles in the final
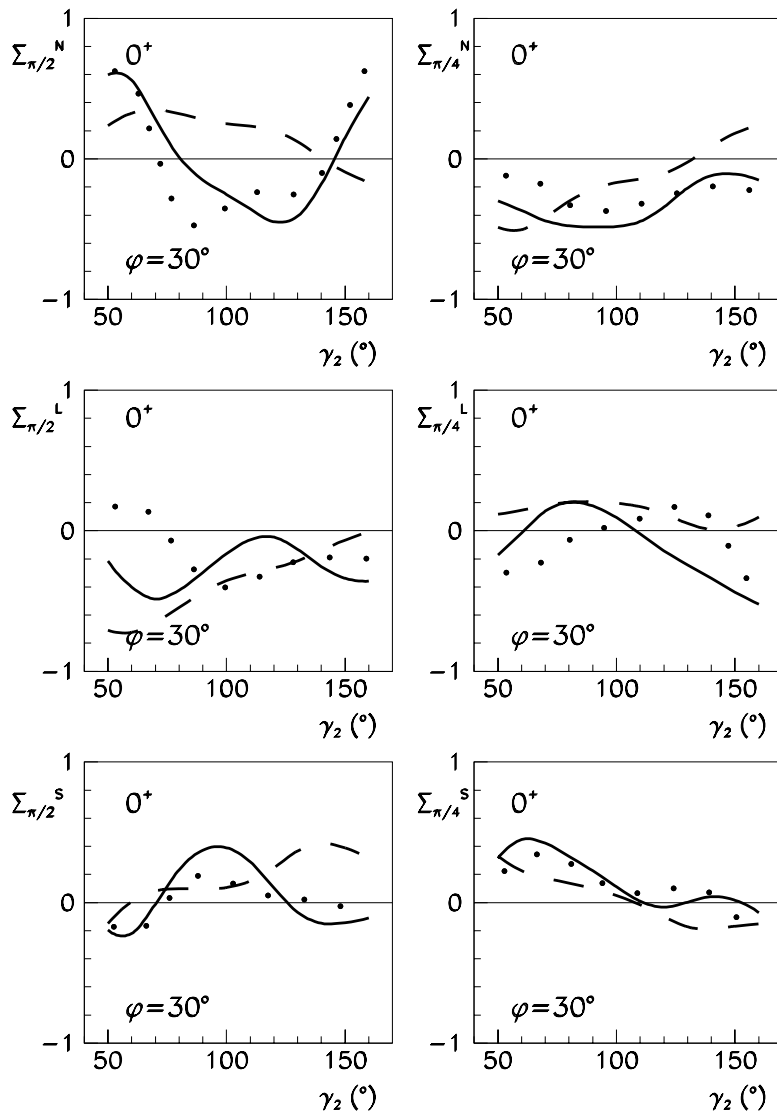
Fig. 16. The polarization observables $\Sigma^N_{\pi/2}$, $\Sigma^N_{\pi/4}$, $\Sigma^L_{\pi/2}$, $\Sigma^L_{\pi/4}$, $\Sigma^S_{\pi/2}$, and $\Sigma^S_{\pi/4}$ for the same reaction and in the same conditions and kinematics as in fig. 13. Line convention as in the upper panel of fig. 10.

state, that are neglected in the present model. For the kinematics that are usually considered these effects should not be large in the cross-section, but might be emphasized in particular polarization observables.

5 Summary and conclusions

Two-nucleon knockout reactions represent the best suited tool for exploring the behaviour of nucleon pairs in nuclei and their mutual interaction. In particular, electromagnetic reactions give a direct access to nuclear structure and correlations. A combined analysis of cross-sections and polarization observables is required for this study.

In this paper we have given the general properties of the $(\vec{\gamma}, \vec{N}N)$ reaction where the incident photon is linearly or circularly polarized and the polarization of one outgoing nucleon is detected. In the most general situation 16 measurable quantities, including the cross-section, are obtained, each one corresponding to one different structure

function. These observables allow a complete investigation of all the components and the properties of the hadron tensor.

For a complete determination an out-of-plane kinematics is needed, *i.e.* a kinematics where one nucleon does not lie on the plane of the photon and of the other nucleon. In the more usual coplanar kinematics a situation similar to the one of the $(\vec{\gamma}, \vec{N})$ reaction is recovered, and only 8 observables are nonvanishing.

Ten structure functions, and therefore the corresponding observables, vanish when the PW approximation is considered for the outgoing nucleons. These quantities appear very well suited to investigate the effect of FSI between the ejected nucleons and the residual nucleus, and, possibly, the mutual interaction between the two outgoing nucleons.

Numerical examples have been presented for the exclusive $^{16}O(\gamma, np)^{14}N$ and $^{16}O(\gamma, pp)^{14}C$ reactions. ^{16}O is a well suited target for this investigation. From the theo-

retical point of view, a great deal of work has been done and a large experience has been acquired on this nucleus. From the experimental point of view, precise measurements have been already carried out for these reactions or are planned in different laboratories, aiming at determining cross-sections and polarization observables for individual final states. It is of particular interest to consider exclusive reactions. Previous investigations have shown that different final states exhibit a different sensitivity to the theoretical ingredients of the calculations and to the various reaction processes. Thus, the experimental resolution of specific final states may act as a filter to disentangle and separately investigate different reaction processes and, in particular, to study nuclear correlations.

The results are very sensitive to the treatment of the nucleon pair wave function and to different aspects involving nuclear structure and correlations. The comparison of theoretical predictions with experimental data can thus impose severe constraints to the theoretical models. The polarization measurements, which are here particularly addressed, are expected to be sensitive to the small components of the transition amplitudes, which do not show up in the cross-sections, where they are generally overwhelmed by the dominant components.

In this paper cross-sections and polarization observables of the $^{16}O(\gamma, np)^{14}N$ and $^{16}O(\gamma, pp)^{14}C$ reactions have been calculated with a similar approach and considering the transitions to the ground state of the residual nucleus. The nuclear current contains a one-body part, which contributes to the transition only through the correlations, and a two-body part, given by the pion seagull, the pion-in-flight and the Δ isobar contributions for (γ, np) reactions, and only by the contribution of the Δ without charge exchange for (γ, pp) reactions. In the np pair wave function the effects of short-range and tensor correlations are taken into account, while the pp pair includes a consistent treatment of short-range and long-range correlations.

As an example, a photon energy of 120 MeV, which seems suitable for experiments, has been chosen in the calculations. At this energy value the Δ plays only a minor role. Thus, in the $^{16}O(\gamma, np)^{14}N$ reaction the seagull current is dominant. The contribution of the one-body current is not very important in general, but can be meaningful in particular situations. The contribution of tensor correlations is significant, particularly at high values of the recoil momentum. Both the one-body and the Δ current are important in the $^{16}O(\gamma, pp)^{14}C$ reaction. The relevance of either contribution can be emphasized in particular kinematic conditions and in different observables.

The polarization observables are always sizable. They are sensitive to all the different terms of the nuclear current and also to their interference. A combined experimental determination of cross-sections and polarizations would give a complete information on the reaction process and result in a stringent test of the theoretical models. This would make it possible to disentangle the different contributions to the reactions and shed light on the genuine nature of correlations in nuclei.

References

1. K. Gottfried, Nucl. Phys. **5**, 557 (1958); Ann. Phys. (N.Y.) **21**, 63 (1963).
2. S. Boffi, C. Giusti, F.D. Pacati, M. Radici, *Electromagnetic Response of Atomic Nuclei, Oxford Studies in Nuclear Physics* (Clarendon Press, Oxford, 1996).
3. J. Arends, J. Eyimk, H. Hartmann, A. Hegerath, B. Mecking, G. Nöldeke, H. Rost, Z. Phys. A **298**, 103 (1980).
4. M. Kanazawa, S. Homma, M. Koike, Y. Murata, H. Okuno, F. Soga, N. Yoshikawa, A. Sasaki, Phys. Rev. C **35**, 1828 (1987).
5. J.C. McGeorge, I.J.D. MacGregor, S.N. Dancer, J.R.M. Annand, I. Anthony, G.I. Crawford, S.J. Hall, P.D. Harty, J.D. Kellie, G.J. Miller, R.O. Owens, P.A. Wallace, D. Branford, A.C. Shotter, B. Schoch, R. Beck, H. Schmieden, J.M. Vogt, Phys. Rev. C **51**, 1967 (1995) ; P. Grabmayr, J. Ahrens, J.R.M. Annand, I. Anthony, D. Branford, G.E. Cross, T. Davinson, S.J. Hall, P.D. Harty, T. Hehl, J.D. Kellie, Th. Lamparter, I.J.D. MacGregor, J.A. MacKenzie, J.C. McGeorge, G.J. Miller, R.O. Owens, M. Sauer, R. Schneider, K. Spaeth, G.J. Wagner, Phys. Lett. B **370**, 17 (1996); P.D. Harty, I.J.D. MacGregor, P. Grabmayr, J. Ahrens, J.R.M. Annand, I. Anthony, R. Beck, D. Branford, G.E. Cross, T. Davinson, S.J. Hall, T. Hehl, R.O. Owens, M. Sauer, R. Schneider, K. Spaeth, Phys. Lett. B **380**, 247 (1996); Th. Lamparter, J. Ahrens, J.R.M. Annand, I. Anthony, R. Beck, D. Branford, G.E. Cross, T. Davinson, P. Grabmayr, S.J. Hall, P.D. Harty, T. Hehl, J.D. Kellie, I.J.D. MacGregor, J.A. MacKenzie, J.C. McGeorge, G.J. Miller, R.O. Owens, M. Sauer, R. Schneider, K. Spaeth, G.J. Wagner, Z. Phys. A **355**, 1 (1996); I.J.D. MacGregor, T.T-H. Yau, J. Ahrens, J.R.M. Annand, R. Beck, D. Branford, P. Grabmayr, S.J. Hall, P.D. Harty, T. Hehl, J.D. Kellie, Th. Lamparter, M. Liang, J.A. MacKenzie, S. McAllister, J.C. McGeorge, R.O. Owens, J. Ryckebusch, M. Sauer, R. Schneider, D.P. Watts, Phys. Rev. Lett. **80**, 245 (1998); D.P. Watts, I.J.D. MacGregor, J. Ahrens, J.R.M. Annand, R. Beck, D. Branford, P. Grabmayr, S.J. Hall, P.D. Harty, T. Hehl, J.D. Kellie, Th. Lamparter, M. Liang, J.A. MacKenzie, S. McAllister, J.C. McGeorge, R.O. Owens, M. Sauer, R. Schneider, G.J. Wagner, T.T-H. Yau, Phys. Rev. C **62**, 014616 (2000).
6. L. Isaksson, Ph.D. thesis, University of Lund (1996); L. Isaksson, J.-O. Adler, B.-E. Andersson, K.I. Blomqvist, A. Sandell, B. Schröder, P. Grabmayr, S. Klein, G. Mauser, A. Mondry, J.R.M. Annand, G.I. Crawford, V. Holliday, J.C. McGeorge, G.J. Miller, Phys. Rev. Lett. **83**, 3146 (1999).
7. J. Ahrens, J.R.M. Annand, R. Beck, D. Branford, P. Grabmayr (spokesperson), S.J. Hall, T. Hehl, D.J. Ireland, J.D. Kellie, I.J.D. MacGregor, M. Mayer, J.C. McGeorge, F.A. Natter, R.O. Owens, M. Sauer, G.J. Wagner, S. Wunderlich, MAMI proposal Nr: A2/4-97.
8. P. Grabmayr, *Proceedings of the Fourth Workshop on Electromagnetically Induced Two-Nucleon Emission, Granada, 1999*, edited by C. Garcia-Recio, P. Grabmayr, A.M. Lallena and R. Owens (University of Granada, Granada, 1999) p. 331.
9. C. Giusti, F.D. Pacati, Nucl. Phys. A **641**, 297 (1998).

10. J. Ryckebusch, D. Debruyne, W. Van Nespen, Phys. Rev. C **57**, 1319 (1998).

11. C.J.G. Onderwater, K. Allaart, E.C. Aschenauer, Th.S. Bauer, D.J. Boersma, E. Cisbani, S. Frullani, F. Garibaldi, W.J.W. Geurts, D. Groep, W.H.A. Hesselink, M. Iodice, E. Jans, N. Kalantar-Nayestanaki, W.-J. Kasdorp, C. Kormanyos, L. Lapikás, J.J.van Leeuwe, R. De Leo, A. Misiejuk, A.R. Pellegrino, R. Perrino, R. Starink, M. Steenbakkers, G. van der Steenhoven, J.J.M. Steijger, M.A. van Uden, G.M. Urciuoli, L.B. Weinstein, H.W. Willering, Phys. Rev. Lett. **78**, 4893 (1997).

12. C.J.G. Onderwater, K. Allaart, E.C. Aschenauer, Th.S. Bauer, D.J. Boersma, E. Cisbani, W.H. Dickhoff, S. Frullani, F. Garibaldi, W.J.W. Geurts, C. Giusti, D. Groep, W.H.A. Hesselink, M. Iodice, E. Jans, N. Kalantar-Nayestanaki, W.-J. Kasdorp, C. Kormanyos, L. Lapikás, J.J. van Leeuwe, R. De Leo, A. Misiejuk, H. Müther, F.D. Pacati, A.R. Pellegrino, R. Perrino, R. Starink, M. Steenbakkers, G. van der Steenhoven, J.J.M. Steijger, M.A. van Uden, G.M. Urciuoli, L.B. Weinstein, H.W. Willering, Phys. Rev. Lett. **81**, 2213 (1998).

13. R. Starink, M.F. Van Batenburg, E. Cisbani, W.H. Dickhoff, S. Frullani, F. Garibaldi, C. Giusti, D.L. Groep, P. Heimberg, W.H.A. Hesselink, M. Iodice, E. Jans, L. Lapikás, R. De Leo, C.J.G. Onderwater, F.D. Pacati, R. Perrino, J. Ryckebusch, M.F.M. Steenbakkers, J.A. Templon, G.-M. Urciuoli, L.B. Weinstein, Phys. Lett. B **474**, 33 (2000).

14. G. Rosner, *Conference on Perspectives in Hadronic Physics*, edited by S. Boffi, C. Ciofi degli Atti, M.M. Giannini (World Scientific, Singapore, 1998) p. 185; *Proceedings of the 10th Mini-Conference on Studies of Few-Body Systems with High Duty-Factor Electron Beams*, edited by H.P. Block, E. Jans, G. van der Steenhoven (NIKHEF, Amsterdam, 1999) p. 95; M. Kahrau, Ph.D thesis, Johannes Gutenberg Universität, Mainz (1999).

15. C. Giusti, F.D. Pacati, K. Allaart, W.J.W. Geurts, W.H. Dickhoff, H. Müther, Phys. Rev. C **57**, 1691 (1998).

16. C. Giusti, H. Müther, F.D. Pacati, M. Stauf, Phys. Rev. C **60**, 054608 (1999).

17. A. Nadasen, P. Schwandt, P.P. Singh, W.W. Jacobs, A.D. Bacher, P.T. Debevec, M.D. Kaichuk, J.T. Meek, Phys. Rev. C **23**, 1023 (1981).

18. J.R.M. Annand, P. Bartsch, D. Baumann, J. Becker, R. Böhm, D. Branford, S. Derber, M. Ding, I. Ewald, K. Föhl, J. Friedrich, J.M. Friedrich, P. Grabmayr (spokesperson), T. Hehl, D.G. Ireland, P. Jennewein, M. Kahrau, D. Knödler, K.W. Krygier, A. Liesenfeld, I.J.D. MacGregor, H. Merkel, K. Merle, P. Merle, U. Müller, H. Müther, A. Natter, R. Neuhausen, Th. Pospischil, G. Rosner (spokesperson), H. Schmieden, A. Wagner, G.J. Wagner, Th. Walcher, M. Weis, S. Wolf, MAMI proposal Nr: A1/5-98.

19. C. Giusti, F.D. Pacati, M. Radici, Nucl. Phys. A **546**, 607 (1992); S. Boffi, C. Giusti, F.D. Pacati, M. Radici, Nucl. Phys. A **564**, 473 (1993).

20. D.J. Tedeschi, G.S. Adams, G. Audit, H. Baghaei, A. Caracappa, W.B. Clayton, A. D'Angelo, M.A. Duval, G. Giordano, S. Hobit, O.C. Kistner, J.M. Laget, R. Lindgren, G. Matone, L. Miceli, W.K. Mize, M. Moinester, C. Ruth, A. Sandorfi, C. Schaerf, R.M. Sealock, L.C. Smith, P. Stoler, P.K. Teng, C.E. Thorn, S.T. Thornton, K. Vaziri, C.S. Whisnan, E.J. Winhold, Phys. Rev. Lett. **73**, 408 (1994).

21. H. Baghaei, *Proceedings of the Second Workshop on Electromagnetically Induced Two-Nucleon Emission, Gent, 1995*, edited by J. Ryckebusch and M. Waroquier (University of Gent, Gent, 1995) p. 195.

22. S. Franczuk, I.J.D. MacGregor, J. Ahrens, J.R.M. Annand, J.F. Arneil, R. Beck, D. Branford, P. Grabmayr, S.J. Hall, T. Hehl, P.D. Harty, D.G. Ireland, J.D. Kellie, K. Livingston, J.C. McGeorge, F.A. Natter, S. Oberkirsch, R.O. Owens, C.J.Y. Powrie, J. Ryckebusch, M. Sauer, A. Settele, P.D. Watts, Phys. Lett. B **450**, 332 (1999); I.J.D. MacGregor, *Proceedings of the Fourth Workshop on Electromagnetically Induced Two-Nucleon Emission, Granada, 1999*, edited by C. Garcia-Recio, P. Grabmayr, A.M. Lallena and R. Owens (University of Granada, Granada, 1999) p. 339.

23. J. Ryckebusch, W. Van Nespen, D. Debruyne, Phys. Lett. B **441**, 1 (1998).

24. C. Giusti, F.D. Pacati, Phys. Rev. C **61**, 054617 (2000).

25. A. Picklesimer, J.W. Van Orden, Phys. Rev. C **35**, 266 (1987).

26. R.B. Wiringa, R.A. Smith, T.L. Ainsworth, Phys. Rev. C **29**, 1207 (1984).

27. C.C. Gearhart, Ph.D thesis, Washington University, St. Louis (1994); C.C. Gearhart, W.H. Dickhoff, private communication.

28. P. Wilhelm, H. Arenhövel, C. Giusti, F.D. Pacati, Z. Phys. A **359**, 467 (1997).

29. W.J.W. Geurts, K. Allaart, W.H. Dickhoff, H. Müther, Phys. Rev. C **54**, 1144 (1996).

30. P. Wilhelm, J.A. Niskanen, H. Arenhövel, Nucl. Phys. A **597**, 613 (1996).